



Rheological behavior in the transient state of PP/EPDM blends with carbon nanofillers

Roberto Zitzumbo-Guzman¹ · Felipe Avalos-Belmontes² · Luis F. Ramos-De Valle³ · Jose C. Ortiz-Cisneros² · Sergio Alonso-Romero¹ · Anayansi Estrada-Monje¹

Received: 25 September 2017 / Revised: 22 February 2018 / Accepted: 14 March 2018 / Published online: 26 March 2018
© Springer-Verlag GmbH Germany, part of Springer Nature 2018

Abstract

The rheological properties in the transient state of PP/EPDM blends with carbon nanofillers had been studied. The carbon nanofillers were incorporated into molten EPDM in an internal mixer at 150 °C. The rheological variables were determined in rotational rheometry at constant temperature of 200 °C. The results suggest that the magnitude of the difference of the normal stress differences (N_1-N_2) of PP/EPDM blends through the time, with and without nanofillers, and has a transition cycle from positive to negative values and vice versa, at constant and at zero shear rate in previously sheared samples. At constant shear rate, the transition cycle is random; meanwhile, it is constant at zero shear rate. This behavior is attributed to the polymeric chain movement, considering that the sheared samples have two molecular reorder processes: an immediate mechanism and another one slower. The fastest reorder process is attributed to the polymeric chains entanglement forming non-stable and stressed molecular structures. In the other hand, the second process is referred to the molecular mobility that takes place inside the stressed entangled polymer, in such a way that its structure tends to molecular stability as the rest time increases.

Keywords Rheological properties · Normal stress differences · PP/EPDM blends · Nanocomposites

Introduction

One of the rheology's objectives is the flux study of the simple fluid. The fundamental variables of the stress of a fluid under the action of a shear field are the shear viscosity and the first and second difference of normal stresses (N_1 and N_2).

The shear viscosity can be measured by shear or elongational flow, while the first and second difference of normal stresses is measured by rotational rheometry. The difference of the normal stress differences (N_1-N_2), can be measured

with parallel plate geometries, while the N_1 with cone/plate geometry (Jensen and Christiansen 2008).

This technique has the disadvantage that when the values of N_1 and N_2 reached a maximum value, a fracture of the melt is produced and the polymer flows out of the geometry. For molten polymers, that fracture occurs at a shear rate of about 10 s^{-1} .

In the case of isotropic materials, the magnitude of the first normal stress difference N_1 is larger than the second normal stress difference N_2 , which normally has a negative value.

Difference of normal stress differences is associated with anisotropy induced by deformation in a fluid. In polymeric liquids, the anisotropy arises from the molecules loss of equilibrium.

The N_1 is responsible for the tendency of the polymer chains of climbing the rod that shears the viscoelastic material and the swelling of the molten polymers extruded at the exit of the die. That is, N_1 is the force that pushes the contact surfaces perpendicular to the flow. The behavior to the first shear difference is the measure of the elasticity, affected by shear stress as a result of molecular morphological alterations in the nanostructure of the material (Narimissa et al. 2014).

More than three decades ago, Kiss and Porter (Kiss and Porter 1978) were the first to show experimental evidence that the

✉ Anayansi Estrada-Monje
aestrada@ciatec.mx

¹ CIATEC A.C., 201 Omega, Industrial Delta, 37545 Leon, GTO, Mexico

² Facultad de Ciencias Químicas, Universidad Autónoma de Coahuila (FCQ-UAC), V. Carranza y González Lobo s/n, 25000 Saltillo, COAH, Mexico

³ CIQA, 140 Blvd. Enrique Reyna, Col. San José de los Cerritos, 25294 Saltillo, COAH, Mexico

magnitude of the first difference of normal stresses could be positive and negative in the same test for lyotropic liquid crystal polymers (LCPs). Time later, Marrucci and Guido (Marrucci and Guido 1995) were the first to widely explain the mechanism of negative normal stress, this matter still arouses great interest between the scientific making rheological studies (Tao et al. 2006).

It has been reported in the literature that in a heterogeneous shear flow (Mall-Gleissle et al. 2002) carried out on the cutting rheometer equipped with parallel plate geometry, shear stresses and the difference of normal stress differences can be determined according to the following equations:

$$\tau_{pp} = \frac{M}{2\pi R^3} \left[3 + \frac{d \ln M}{d \ln \gamma_R} \right] \quad (1)$$

$$N_1 = \frac{2F_z}{\pi R^2} \quad (2)$$

$$N_1 - N_2 = \frac{F_z}{\pi R^2} \left[2 + \frac{d \ln F_z}{d \ln \gamma_R} \right] \quad (3)$$

$$\gamma_R \equiv \frac{\Omega R}{\dot{\Gamma}} \quad (4)$$

where, M is the applied torque, R is the radius of the plates, $\dot{\Gamma}$ is the gap, γ_R is the maximum shear rate at the edge of the geometry, and F_z is the axial thrust force exerted on the geometry.

The dynamic storage and loss module measurements have been determined according to the following equations (Morrison 2001):

$$G' = \frac{IM \cos \delta}{\pi R^4 \theta} \quad (5)$$

$$G'' = \frac{IM \sin \delta}{\pi R^4 \theta} \quad (6)$$

where δ is the phase angle and θ is the angular displacement.

For the other hand, it is well known that the rheological properties of the polymers strongly depend on the internal structure of the material (Luo et al. 2015), which may be modified by fillers, morphology, and the melt processes' history which they have been subjected, among others.

In addition, the large ratio and attractive potential of the inter-particle interactions of the carbon nanotubes can lead to an increase of unwanted effects, such as mechanical entanglement and flow-induced clusters when nanocomposites are under an external shear stress (Hobbie and Fry 2007).

In this paper, the rheological properties in the transient state of a PP/EPDM blend loaded with carbon nanoparticles are discussed. The experimental evidence at constant shear rate dependent on the rest time of the transition cycle from positive to negative values and vice versa of difference of the normal stress differences is also discussed. It is worth mentioning that the investigations reported in the literature, related to measurement of difference of the normal stress differences, have been carried out by varying the shear rate.

Experimental

Isotactic polypropylene (PP) (melt temperature of 162 °C and density of 0.9 g/cm³) was supplied by Dow Chemical, under the trade name Dow H700-12. Ethylene-propylene-diene rubber (EPDM), with ethylidene norbornene as termonomer (4.4%) and propylene content of about 27%, was medium molecular weight. A maleic anhydride-grafted polypropylene was used as coupling agent, grafted with less than 1% of maleic anhydride (PP-g-MA), supplied by DuPont under the trade name of FUSABOND PMD-511D PP-MA.

Graphene carbon nanoplaques (GNP) and 5.58% of ions-OH functionalized multiple wall nanotubes (MWNTCs) were used as nanofillers supplied by TIMESNANO under the trade names of TNIGNP and TNMH1, respectively. The sample composition is shown in Table 1.

Nanocomposites preparation

The compounding was carried out in a Brabender internal mixer with two high shear Banbury type rotors, at 150 °C and 60 rpm for 20 min. Along this period of time, a constant value of the torque was obtained. The nanofillers were added and mixed into the molten EPDM in a ratio of 1:1 w/w.

In another operation, PP, EPDM and PP-g-MA, and the compound obtained before (EPDM/nanofiller) were mixed, extruded in a double screw extruder, and injected to obtain test samples for the characterization.

Rheological properties

The rheometer used for the measurements is a Paar Physica MCR 300 equipped with a thermal chamber CTD 600 and parallel plate geometry with 25 mm of diameter, and the gap was 1 mm at a constant temperature of 200 °C. The dynamic frequency sweeps were performed in a frequency range of 0.01–100 s⁻¹, using a deformation amplitude of 4%. The viscoelastic region was determined by multiple strain sweep measurements to assure that the strain used is within the linear viscoelastic region.

Table 1 This table shows the compositions of the samples studied

No.	PP	EPDM	PP-g-MA	MWNTC's	GNP
1	60	40	2	–	–
2	60	40	2	0.5	–
3	60	40	2	1	–
4	60	40	2	2	–
5	60	40	2	2	0.5
6	60	40	2	2	2

MWNTCs multiple wall carbon nanotubes, GNP graphene nanoplates

For transient experiments, the samples were subjected to a previous deformation, as shown below: First, the samples were sheared for 300 s at a predetermined shear rate, $\dot{\gamma}$. Thereafter, the shear is no longer applied and the samples held at rest for a given time interval, t . Finally, the sample is sheared in the same direction of the previous shear at the same shear rate $\dot{\gamma}$ for 300 s, monitoring the shear stress, elastic recovery, and the difference of the normal stress differences N_1-N_2 during the rest period and the last period of shear.

For the transient test, the rates of shear, $\dot{\gamma}$, were 0.01 and 0.1 s^{-1} , and the rest times were $t = 0, 300, 900,$ and 1700 s.

Results and discussion

The behavior in the transition state of samples 1 and 3 (0 and 1% by weight of carbon nanotubes) is shown in Fig. 1. After the samples have been sheared and let them rest for predetermined times, the shear stress against the shear time at constant shear rate was plotted.

In general, it is observed that the samples, subjected to the same shear rate, have curves with similar shapes. That is, the shapes of the curves of Fig. 1a and Fig. 1c and Fig. 1b and Fig. 1d are similar to 0.01 and 0.1 s^{-1} , respectively.

It is also observed that in the samples under high shear rates (Fig. 1b, d), the peak of shear stress is bigger and better defined.

At the highest shear rate, it is observed that the curves, after reaching a maximum value of the shear stress, fall drastically, to an asymptotic value for all samples, except for those samples that did not have rest time.

The decay of the curves is more drastic in the samples that had more rest time. In the curves of Fig. 1, it can be seen that the maximum value of the shear stress of sample 3 is lower than that observed for sample 1, at both shear rates and for all rest times, except for the samples without rest time.

For samples with no rest time, the shear stress value lacks maximum peak and the curves tend to decrease slightly over the measurement time at constant shear rate.

The rheological behavior of the curves shown in Fig. 1 indicates that after the shear imposed on the molten polymer ceases, there is a process of mobility of polymer chains inside the nanocomposite that tends to form molecular structures (Zitzumbo-Guzman et al. 2006).

If it is accepted that the more stable molecular structures require more effort to deagglomerate than ones less stable structures, then it may be said that there is formation of structural conformations inside the nanocomposite and these are becoming more stable as the rest time increases. That is, after

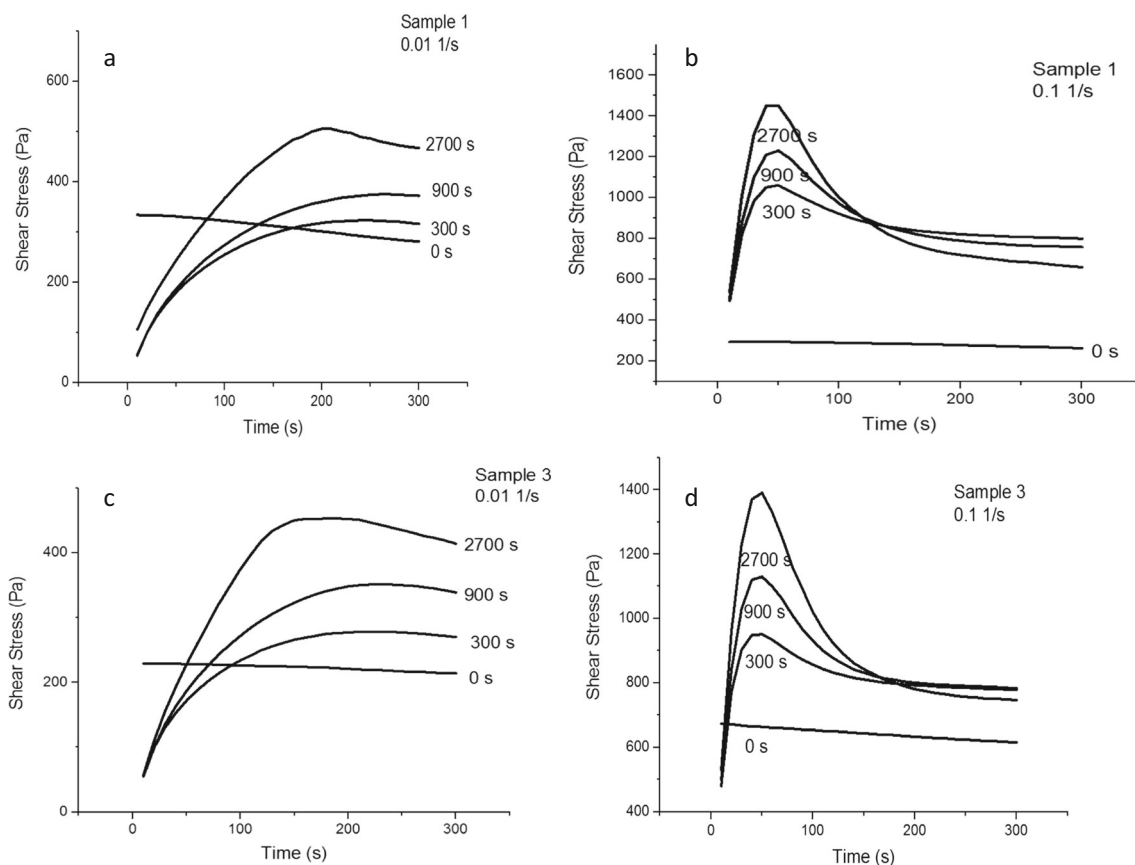


Fig. 1 a–d The shear stress against the shear time at constant shear rate

the shear ceases, there are two processes of molecular rearrangement, an immediate mechanism and another one slower.

The first process could be the elastic recovery with polymeric chains entanglement forming unstable molecular structures. These unstable molecular structures are under stress due to the elastic torsion bar generated during its sudden formation; meanwhile, the second reordering process could be referred to the molecular mobility into the entanglement polymer, which structure gets stronger with the rest time. This could explain the fact that when the materials are re-sheared, shear stress increases until they break the formed structures. After reaching the maximum shear stress, shear stress decreasing is inevitable because the material loses all of the acquired structure. The drop in shear stress is most pronounced in the samples with the longest rest time and larger shear.

For the other hand and according to Newton's viscosity law $\sigma = \eta \times \dot{\gamma}$, it may be said that at constant shear rate, the plotted stress in Fig. 1 is the polymer viscosity.

The viscosity versus time curves and the shear stress curves against shear time are qualitatively similar in shape (the curves are not shown for obvious reasons).

According to the above deduction, when a sample is sheared and the shear ceases for a given time, its viscosity increases as the rest time increases. That is, when the shear imposed on the molten polymer ceases, a process of molecular mobility begins that causes conformational changes in the internal structure of the polymer, increasing its viscosity with the rest time.

Increases in shear viscosity have been reported in tomato juice with soybean (Tiziani and Vodovotz 2005), where the juice exhibits a thixotropic behavior at low shear rates, followed by a transition to the rheopectic behavior at higher shear rates.

On the other hand, it has been found in the literature (Takahashi et al. 1999) reports with similar results in elongational flow, which have been called hardening behavior with the deformation. These researchers found that high molecular weight polymers exhibit a hardening behavior with elongational flow deformation, which was attributed to the existence of a long time relaxation mechanism and large values of the damping function. However, they themselves found that in blends of immiscible polymers, which exhibit long relaxation times, the blends do not show considerable hardening with deformation.

In Fig. 2, the slope obtained from shear stress curves against shear time at the beginning of shear, with respect to the carbon nanofiller concentration (CNPs), was plotted in samples with a rest time of 2700 s.

If it is assumed that the slope of the stress curves against shear time represents the stability of the structure formed by the shear, according to the explanation above, it may be said that the increase of carbon nanofiller in the nanocomposite

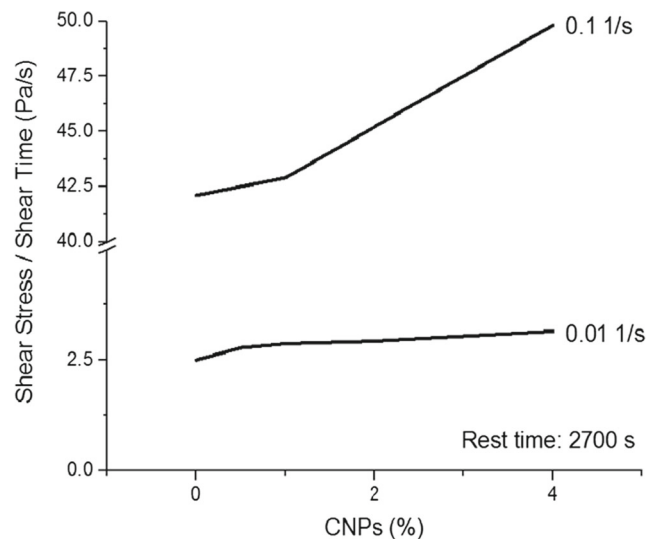


Fig. 2 The slope obtained from the onset of the shear stress curves against shear time, with respect to the carbon nanocarbon concentration, at a rest time of 2700 s

causes the formation of more stable structures inside the material. Thus, the stability of the internal structures of the studied samples is more affected by the shear rate at which the samples are subjected than the load content in the nanocomposite matrix.

In Fig. 3, the strain % against the rest time is plotted, during 2700 s of rest. It is worth mentioning that at rest times less than 2700 s, the strain of the samples does not reach asymptotic values.

After the shear stress applied to the samples ceases, it is observed that during the rest time, the stress relaxation of the material subjected to low shear flow rates reaches asymptotic values (Fig. 3a). While the stress relaxation of samples with larger shear history reaches constant stress relaxation values (Fig. 3b).

In Fig. 3, it is observed that relaxation of the strain of the deformed polymer at low shear rates is softer compared to the deformed samples at larger shear rates measured by steps. In addition, the stress relaxation of nanocomposites that were deformed at low shear rates (Fig. 3a) is 35 versus 2% of the deformed samples at higher shear rates (Fig. 3b).

Nanocomposites with higher nanocarbon content have a lower percentage of stress relaxation than less loaded nanocomposites.

The rheological behavior of the samples of Fig. 3b could be due to the fact that the polymer chains reach a greater degree of stretching, in such a way that when shear ceases, the formation of the material structure is so rapid that it could undergo molecular slip over the walls of the geometry of parallel plates. If this assertion is accepted, then it may be said that in the structures formed, stresses are retained and these are responsible for keeping the sample stressed. That is, the energy absorbed by the sample during shearing is not totally

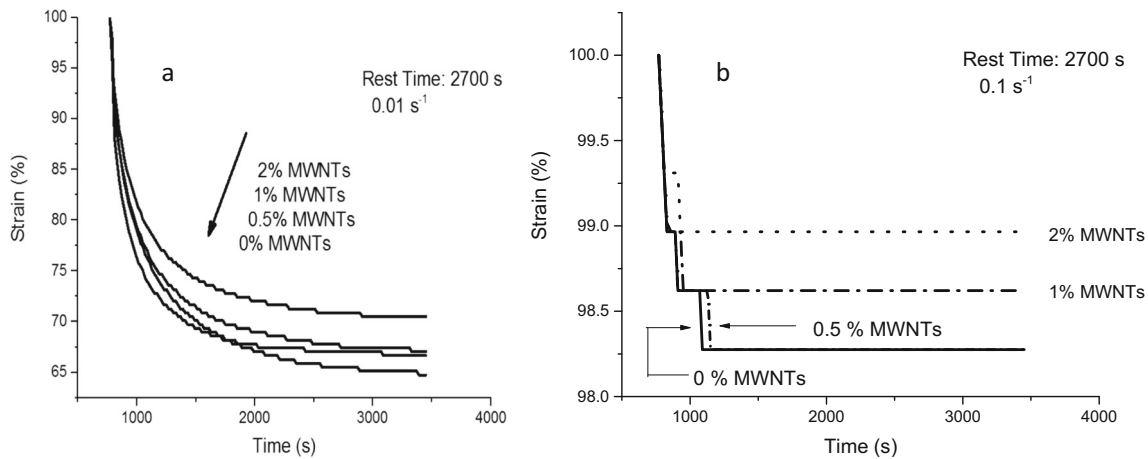


Fig. 3 The stress percentage against the rest time, during 2700 s of rest. The samples were subjected to constant shear of 0.01 and 0.1 s⁻¹ for **a** and **b**, respectively

dissipated when the shear ceases and the structure of the material retains that energy by keeping the sample stressed.

The elastic recovery and molecular entanglement of the polymer chains in samples that have been sheared at large shear rate are carried out by molecular sliding over the wall of the parallel plates intermittently. In contrast, when the shear flow is carried out at low shear rate (Fig. 3a), the polymer chains are not strongly extended, in such a way that the elastic recovery and the molecular entanglement of the polymer chains form a little stressed structure without the presence of molecular slip over the walls of the geometry.

In Fig. 4, the difference of the normal stress differences ($N_1 - N_2$) against the shearing time is plotted. First, the samples were sheared and immediately thereafter they were put to rest for various predetermined times, recording the difference of normal stresses after the rest time at constant shear rate.

Figure 4a shows that the curve with 900 s of rest time and shear rate of 0.1 s⁻¹ presents a drop of $N_1 - N_2$. The sudden drop in the values of the difference of the normal stress differences

to a negative maximum is referred as the tumbling down or collapse.

Figure 4b shows that the curves with 0 and 300 s of rest and shear rate of 0.01 s⁻¹ presented a collapse of $N_1 - N_2$. All these collapses are random and hardly occur in the same way; that is, they are not repetitive.

It should be mentioned that the first difference of normal stresses with negative values (when N_1 collapses) has already been reported and explained in liquid crystal polymers (LCPs) by other authors (Kiss and Porter 1978; Marrucci and Guido 1995). Marrucci and Guido (Marrucci and Guido 1995) concluded that the negative normal stress effect is the most important rheological effect that characterizes liquid crystals. The explanation is based on the unstable orientation of the nematic phase of the liquid crystals with the flow (Baek et al. 1993a; Baek et al. 1993b). The conclusion was that the rod-like molecules of liquid crystal polymers induced by shearing may rotate on their own axis. That movement and aligned flow regimes are responsible for the first normal stress

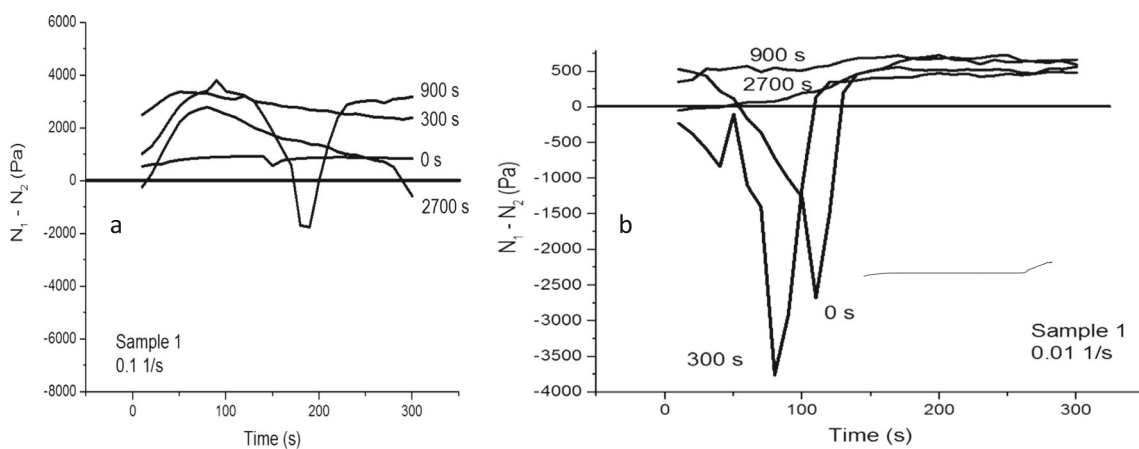


Fig. 4 $N_1 - N_2$ is plotted against the shear time. First, the samples were sheared for 300 s, then they were put to rest during 0, 300, 900, and 2700 s. Subsequently, the samples were sheared at constant rate and the magnitude of $N_1 - N_2$ was recorded **a**) Shear rate of 0.1 1/s and **b**) Shear rate of 0.01 1/s

difference unusual behavior. In such a way that the negative values of the first difference of normal stress (N_1) unequivocally imply that the nematic phase of liquid crystals is the one who is collapsing. Another conclusion reached was that the shear rate range where N_1 is negative marks the dynamic transition of the collapse to alignment by flow.

For the above, surprisingly our results do not depend on the shear rate neither the nematic phase inside the material. We think its explanation is much more complex.

We consider that this behavior of the collapse of the difference of the normal stress differences corresponds more to the inter- and intra-molecular interactions of the macromolecular agglomerates that are formed by the molecular movement of the polymer chains inside the polymers.

We believe that these molecular rearrangements could be due to the stress of the polymer chains acquired during the shearing to which they were subjected, in such a way that the molecular movement will continue until the stress is dissipated.

In Fig. 5, the difference of the normal stress differences against the shearing time is plotted. The samples were first sheared and immediately rested for 2700 s, recording the difference of normal stress after resting at constant shear rate.

The construction of these curves was carried out with three or four repetitions, and in all cases, those samples that showed a collapse of the difference of the normal stress differences were discarded.

In this way, it is observed that the difference of the normal stress differences of the nanocomposites increases to a maximum point for each material and then decreases as the shear time increases at constant rate. Also, as the concentration of carbon nanofillers in the nanocomposite increases, the normal stress difference is lower.

To further investigate the phenomenon of difference of the normal stress differences collapse, we shear the samples for

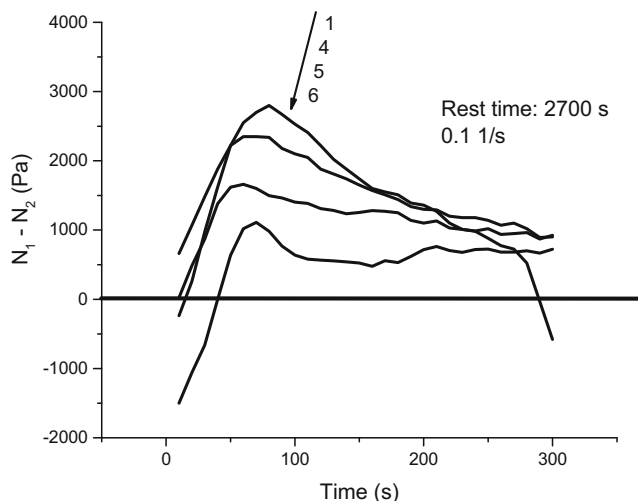


Fig. 5 N_1-N_2 is plotted against shear time. At constant shear rate, the samples with 2700 s of rest were sheared recording the magnitude of N_1-N_2

300 s and stop the shear, recording the difference in normal stress during the rest time.

In Fig. 6, the difference of the normal stress differences against the rest time is plotted. First, the samples were sheared and immediately thereafter they were put to rest during different times and the difference of the normal stress differences was recorded.

In all cases, it was observed that at rest times less than 2700 s, only one curve or none with negative values of N_1-N_2 appears. As the rest time increases, curves with negative values of N_1-N_2 appear. In all our samples, curves are obtained as shown in Fig. 6 (not shown).

In these curves, it is observed how the negative value of the difference of the normal stress differences occurs as the rest time passes. In addition, curves do not always start with positive values, in some cases, they start with negative values and go up or down, depending on the internal structure of the material at the moment in which the N_1-N_2 values are recorded entering to the transition cycle from positives to negatives values and vice versa.

According to the behavior of Fig. 6, it was decided to prolong the rest time to 21,600 s, recording at all times the difference of the normal stress differences. The result is surprising and shown in Fig. 7.

In Fig. 7, it can be seen that the difference of normal stress differences during rest begins with positive values decreasing with time until reaching a negative maximum, then its value increases until reaching a positive maximum and returns again, repeating the cycle of transition from positive to negative values and vice versa. At this point, it should be remembered that curves do not always begin with positive values, as we discussed above.

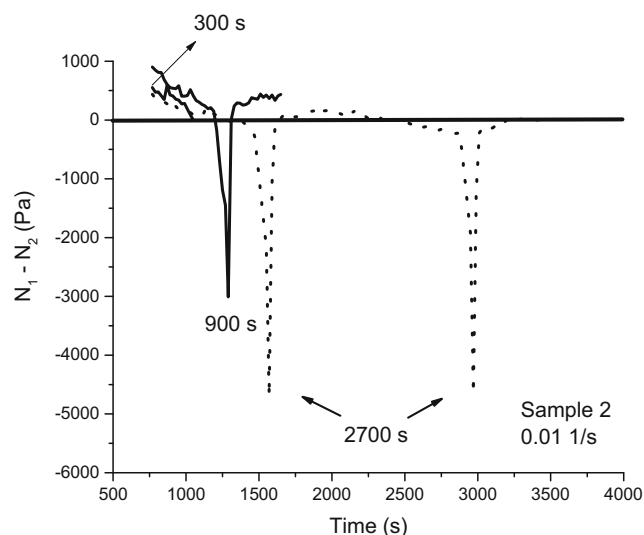


Fig. 6 N_1-N_2 is plotted against the rest time in samples with 2700 s rest. The magnitude of the N_1-N_2 is recorded during rest. Before the resting time, the samples were sheared for 300 s

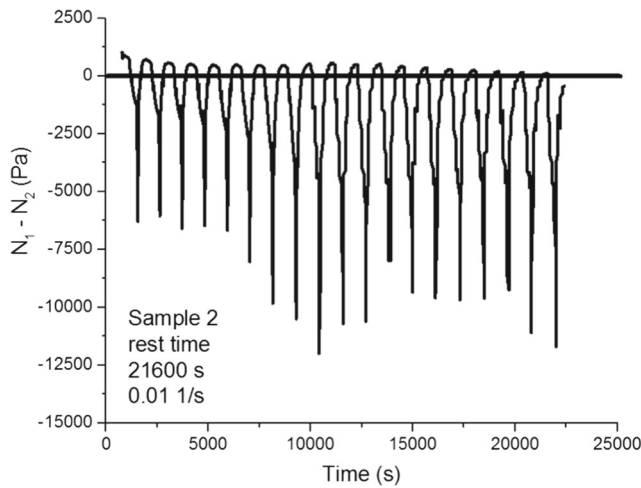


Fig. 7 $N_1 - N_2$ is plotted against the rest time in samples with 21,600 s of rest. The magnitude of the $N_1 - N_2$ is recorded during rest. Before the resting time, the samples were sheared for 300 s

This result could corroborate that the transition cycle from positive to negative values and vice versa could be originated by the second mechanism of mobility, referred to the molecular mobility that takes place inside the entangled polymer, as previously mentioned. Then, it may be possible that the polymer acquires the energy that has been supplied by the shear, in such a way that the polymer chains could be extended and at the moment shear ceased, the polymer has an unstable elastic recovery with the stressed molecular entanglement (immediate mechanism of mobility) and conformational changes in the stressed molecular entanglement (second mechanism of mobility).

The cycle from positive to negative values and vice versa of the difference in normal stresses may have its origin due to the molecular movements. That is, the second mechanism of

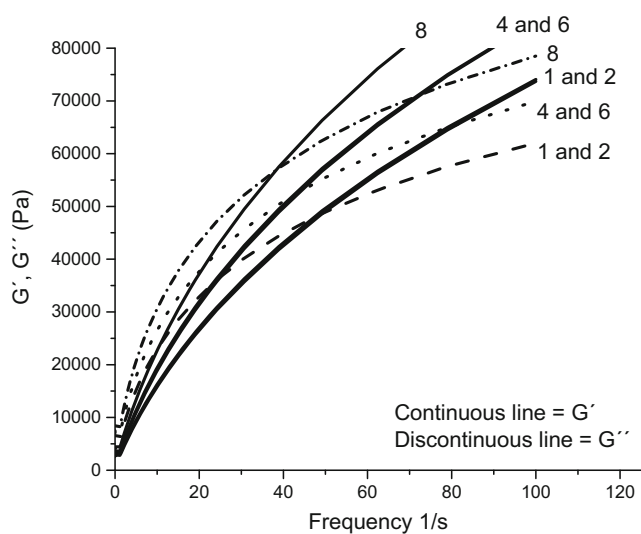


Fig. 8 The storage (G') and loss (G'') modules are plotted against the frequency. The frequencies were from 0.01 to 100 s^{-1}

molecular mobility may be considered as the manifestation of the stress of the material for de-stressing, which is why structural changes occur within the polymer.

It is also observed that the positive values of the difference of normal stress differences during the transition cycle from positive to negative values and vice versa decreases with rest time, until tending to zero, which may be occur after a time of rest of 21,600 s for the studied samples.

On the contrary, the negative values of difference of normal stress differences during the transition cycle from negative to positive values and vice versa exhibit high and low fluctuations with rest time.

It was surprising to find periodicity in the fluctuations from negative to positive values in the transition cycle for the rest period, contrary to the random values found for the sheared samples at constant shear rates (Figs. 4b and 7).

The negative values of the normal stress difference, in absolute terms, are considerably bigger than the positive ones. It could be due to the gravitational forces acting on the material and its adherence to the walls of the parallel plates. In conclusion, this result indicates that the change in the difference of normal stresses from positive to negative values and vice versa is mainly due to the molecular movement of the polymer chains rather than to the shear rate increase, as has been reported in the literature (Jensen and Christiansen 2008).

In Fig. 8, the storage and loss modules, G' and G'' , against the frequency are plotted. At low frequencies, it can be seen that G'' is greater than G' , which implies that nanocomposites have a liquid-like behavior. With frequency increasing, the storage module becomes larger than the loss modulus and the nanocomposites changes to have a solid-like behavior.

The frequency at which G' and G'' are intercepted represents the characteristic time or response time of the material. In Fig. 8, it is observed that the characteristic time of the materials decreases as the nanofiller content increases.

It is also observed in the rheological response of the modules that carbon nanofiller does not form a three-dimensional structural network with the polymer matrix, which implies that they could be inside the nanocomposites as filler and not as reinforcing fillers no matter of the nanoparticle geometry.

Conclusions

Two processes of molecular rearrangement were observed: an immediate mechanism and another one slower, in polymer samples subjected to processes of shearing and rest. In the first one, the elastic recovery with the entanglement of polymer chains may occur, forming stressed and unstable molecular structures, whereas the second could be referred to the molecular mobility occurring inside the entangled polymer, whose structure tends to stabilize as the rest time is increased.

The difference of normal stress differences in the transition cycle from positive to negative values and vice versa during rest time in sheared samples could be due to the second mechanism of molecular mobility, related to the stress experienced by entangled material to suffer the de-stress process.

In the transition cycle of positive and negative values and vice versa, the difference of normal stress differences during the rest time is periodic; meanwhile, the transition cycle is random during the shearing of the samples. In addition, the cycle above mentioned is mainly due to the molecular movement of the polymer chains, rather than the increase of the shear rate.

Acknowledgments We would like to express our great thanks to the National Council of Science and Technology of Mexico (CONACYT) for the financial support given to Dr. R. Zitzumbo to collaborate in this research during his sabbatical stay with the project number 266301 of the 2015 call.

References

- Baek SG, Magda JJ, Cementwala S (1993a) Normal stress differences in liquid crystalline hydroxypropylcellulose solutions. *J Rheol* 37: 935–945
- Baek SG, Magda JJ, Larson RG (1993b) Rheological differences among liquid-crystalline polymers. I. The first and second normal stress differences of PBG solutions. *J Rheol* 37(6):1201–1224
- Hobbie EK, Fry DJ (2007) Rheology of concentrated carbon nanotube suspensions. *J Chem Phys* 126:124907
- Jensen EA, Christiansen J d C (2008) Measurements of first and second normal stress differences in a polymer melt. *J Non-Newtonian Fluid Mech* 148:41–46
- Kiss G, Porter RS (1978) Rheology of concentrated solutions of poly(γ -benzyl-glutamate). *J Polym Sci Polym Symp* 65:193–211
- Luo Y, Xin C, Zheng D, Li Z, Zhu W, Wu S, Zheng Q, He Y (2015) Effect of processing history on the rheological properties, crystallization and foamability of branched polypropylene. *J Polym Res* 22:117
- Mall-Gleissle SE, Gleissle W, McKinley GH, Buggisch H (2002) The normal stress behaviour of suspensions with viscoelastic matrix fluids. *Rheol Acta* 41:61–76
- Marrucci G, Guido S (1995) Shear flow rheology of liquid crystalline polymers. *Int J Polym Anal Charact* 1:191–199
- Morrison FA (2001) *Understanding rheology*. Oxford University Press, New York
- Narimissa E, Rahmanm A, Gupta RK, Kao N, Bhattacharya SN (2014) Anomalous first normal stress difference behavior of polymer nanocomposites and liquid crystalline polymer composites. *Polym Eng Sci* 54(6):1300–1312
- Takahashi T, Takimoto J, Koyama K (1999) Elongational viscosity for miscible and immiscible polymer blends. II. Blends with a small amount of UHMW polymer. *J Appl Polym Sci* 72(7):961–969
- Tao YG, Otter WKD, Briels WJ (2006) Shear viscosities and normal stress differences of rigid liquid-crystalline polymers. *Macromolecules* 39:5939–5945
- Tiziani S, Vodovotz Y (2005) Rheological effects of soy protein addition to tomato juice. *Food Hydrocoll* 19:45–52
- Zitzumbo-Guzman R, Alonso-Romero S, Avalos-Belmonte F, Ortíz-Cisneros JC, López-Manchado MA, Arroyo M (2006) Structural analysis of nanocomposites based on HDPE/EPDM blends. *J Nanosci Nanotechnol* 6(2):331–336

Publisher's Note

Springer Nature remains neutral with regard to jurisdictional claims in published maps and institutional affiliations.